Noninvasive, Nondestructive Measurement of Tomato Concentrate Spoilage in Large-Volume Aseptic Packages

Michele N. Martin, Bruce J. Balcom, Michael J. McCarthy, and Matthew P. Augustine

Abstract: Low frequency nuclear magnetic resonance (NMR) is used to noninvasively and nondestructively detect spoiled tomato concentrate stored in >200 L metal-lined containers. It is shown that longitudinal and transverse NMR relaxation times change as the tomato concentrate spoils. A rapid, viscosity-dependent spoilage detection method that takes advantage of the inherent inhomogeneity in single-sided NMR instruments is proposed. Here, the effective transverse magnetization decay rate is used as a parameter to determine tomato concentrate spoilage. Three different low frequency, single-sided NMR instruments are described and compared to determine the optimum sensor for spoiled tomato concentrate detection in large-format, metal-lined, aseptic containers. The most effective NMR sensor for this application is temperature stable and has large magnetic field gradients and a homogeneous magnetic field region offset >0.5 cm from the magnet surface.

Keywords: aseptic container, NMR, process monitoring, spoilage, tomato concentrate

Practical Application: This manuscript describes a noninvasive and nondestructive tomato concentrate spoilage detector for application to large-format, sealed, commercial storage bins.

Introduction

The United States produces over 10,000,000 tons of processing tomatoes each year. Roughly 90% of these tomatoes are processed in California where the harvest takes place between late July and mid-October. In order to fulfill the tomato demand throughout the entire year, tomatoes are processed into a concentrate and stored in large aseptic totes. These sealed totes are stored outside and exposed to a range of temperatures based on the weather. The tote is constructed from thin sheets of plastic and aluminum laminate material and is essentially a sealed, giant >200 L metal-lined plastic bag. The tomato concentrate is then reprocessed into ketchup, juices, soups, or sauces throughout the remainder of the year (Gould, 2013; Luster, 1978). If, after aseptic packaging, the tomato concentrate is contaminated with trace amounts of microbes, the entire large-volume bin will be susceptible to spoilage as the microbes proliferate during storage. The existing tomato concentrate spoilage detection methods are destructive to the aseptic sample, expensive, and unreliable (Concina et al., 2009; Schenz, Courtney, Israel, & Reaves, 1993). Consequently, the tomato concentrate processing industry has identified the need for a noninvasive sensor that can detect spoilage in large, sealed aseptic totes with a metal reinforcing layer. An effective sensor is noninvasive and able to identify spoiled tomato concentrate while conforming to samples in storage containers of different sizes and geometries. This study develops a low magnetic field, single-sided nuclear magnetic resonance (NMR) instrument in a factory-deployable sensor that can distinguish between pristine and spoiled tomato concentrates in aseptic storage containers. Longitudinal and transverse NMR relaxation times, T_1 and T_2, respectively, were used to monitor spoilage for a variety of different factory-relevant mechanisms, and the performance of three low-frequency, single-sided instruments was compared with the goal of developing the most effective tomato concentrate spoilage detector.

NMR is an analytical technique that noninvasively and nondestructively provides insight into the chemical composition of a sample. The key feature that NMR offers is the ability to study the tomato concentrate in its native, stored environment so that neither the aseptic bag nor the container need to be opened or compromised in any way. Schenz et al. (1993) showed that NMR can be used to noninvasively detect spoilage of nutritional products in thin, nonmetallic aseptic containers. The work presented here extends this idea to an aseptic bag with a metal layer, which is housed inside either a plastic or wooden large-volume bin with a natural 0.5 to 4 cm barrier between the stored product and the NMR sensor. Aseptic packaging involves packing sterile product into sterile containers while in a sterile environment. The aseptic packaging process is attractive to the tomato processing industry because the need for intense postpackaging heat is not required and thus the flavor and color of the product are preserved. Schenz et al. (1993) showed that the T_1 and T_2 values of nutritional products changed upon contamination with various microorganisms. It was similarly shown that for at least one spoilage mechanism, the T_1 value of tomato concentrate increased upon spoilage (Pinter, Harter, McCarthy, & Augustine, 2014). In the first part of the work presented here, the T_1 and T_2 relaxation values of tomato concentrate contaminated by a variety of different factory-relevant spoilage mechanisms were measured in the laboratory to ensure that changing T_1 and T_2 values accurately report spoiled tomato concentrate.

JFDS-2019-0889 Submitted 6/7/2019, Accepted 7/22/2019. *Authors Martin, McCarthy, and Augustine are with the Dept. of Chemistry, Univ. of California, Davis, One Shields Ave., Davis, CA 95616, U.S.A. Author Balcom is with the Dept. of Physics, Univ. of New Brunswick, Fredricton, New Brunswick, E3B 5A3, Canada. Direct inquiries to author Augustine (Email: maugust@ucdavis.edu).*

doi: 10.1111/1750-3841.14778

Journal of Food Science A Publication of the Institute of Food Technologists

The noninvasive, nondestructive nature of single-sided NMR combined with the ability to study different size and geometry samples is what makes single-sided NMR attractive for a variety of food applications. Relaxometry and diffusion measurements have previously been used to measure the fat content in food products such as dairy, fish, ground meat, margarine, and mayonnaise (Guthausen et al., 2004; Petrov, Hay, Mastikhin, & Balcom, 2008; Veliyulin, Mastikhin, Marble, & Balcom, 2008; Veliyulin, van der Zwaag, Burk, & Erikson, 2005). Single-sided NMR has also been used to explore the adulteration of virgin olive oil as well as the water loss during the drying process of pears (Adilettaa et al., 2015; Xu, Morris, Bencsik, & Newton, 2014).

The second part of this manuscript considers how tomato concentrate spoilage in a real factory environment can be measured. An NMR system was made factory deployable with portable electronics and used a single-sided permanent magnet that allows for detection through the standard, 200 to 1,000 L tomato concentrate storage bins by temporarily mounting the portable magnet sensor on the side of the bin. The single-sided sensor differs from a conventional NMR instrument because the sample is not completely surrounded by the radio frequency (rf) coil and NMR magnet. This portable geometry causes the applied magnetic fields to inhomogeneously bathe only a small region of the large sample. A rapid, viscosity-dependent measurement that takes advantage of the inhomogeneous magnetic field of the single-sided instrument is described and used as an NMR spoilage detection parameter.

Tomato concentrate is packaged in a sealed 90-μm thick, plastic-coated, aluminum-lined bag, which is supported inside a 0.5 to 4 cm thick plastic or wooden bin. An effective tomato concentrate spoilage detector must have the ability to noninvasively detect spoilage through both the metal layer and storage bin. At low Larmor frequencies (2 to 20 MHz), applied and detected rf magnetic fields are able to penetrate the aluminum aseptic tote material so that NMR signals can be successfully obtained. At higher Larmor frequencies, where resolution is greater, NMR signals are not observed due to the generation of eddy currents on the surface of the metal, which attenuate the applied and detected rf magnetic field (Augustine, Broz, & Lim, 2016; Pinter et al., 2014). The skin depth is

$$\delta = \sqrt{\frac{2}{\sigma \mu \omega}} \quad (1)$$

where σ is the metal conductivity, μ is the magnetic permeability, and ω is the angular frequency. It is the distance into a metal shield where the amplitude of the magnetic field passing through it is attenuated by a factor of 1/e (Celozzi, Rodolfo, & Lovat, 2008). The inverse relationship between the skin depth and frequency in Eq. 1 indicates that lower frequencies can penetrate further into the metal layer. For example, ^{1}H NMR signals can be observed at a 4 MHz Larmor frequency from the contents of a sealed aluminum beverage container. The use of specialized techniques was shown to enhance the signal by a factor of 20 (Augustine, Broz, & Lim, 2016).

This study furthered the development of a tomato concentrate spoilage detector by determining an NMR parameter that can quickly and successfully determine tomato concentrate spoilage due to a wide range of factory-relevant spoilage mechanisms. To allow usage in a factory setting, three single-sided instruments were examined. The advantages and disadvantages of each instrument were explored with the goal of characterizing the most effective sensor for tomato concentrate spoilage.

Table 1–Characteristics of wild-type tomato concentrate samples.

	%NTSS	
Code	Prepared	Stored
1	26	–
2	26	22.87
3	26	16.43
4	31	–
5	31	19.99
6	37	31.40
7	37	38.65
8	37	44.11
9	31	31.34
10	–	9.01
11	31	22.82
12	37	35.86
13	37	37.06
14	31	26.71
15	28	19.90
16	31	–

Materials and Methods

Twenty-three tomato concentrate samples were received from a California tomato processor. Sixteen of the samples, which will be referred to as wild-type samples, were obtained from different locations throughout the processing facility and may have been exposed to various spoilage sources. The percent natural tomato soluble solids (%NTSS) for each sample is summarized in Table 1; the prepared %NTSS was measured after processing and the stored %NTSS was measured after sample collection of stored tomato concentrate. The %NTSS is a tomato industry parameter that reports on the amount of solid tomato that is dissolved into the tomato serum and is proportional to the macroscopic liquid viscosity of the tomato concentrate (McCarthy, Sacher, & Garvey, 2008). The remaining seven samples were pristine, unspoiled tomato concentrate. Six of the pristine samples were received in sealed mini totes while all the other samples were received in 300-mL plastic bottles.

All laboratory samples were kept on ice for 2 weeks. After 2 weeks, all the samples were removed from the ice and brought to room temperature. At room temperature, a visible amount of mold slowly began to grow on some of the samples. Every other day for 40 days, the T_1 and T_2 relaxation times were measured. Measurements were carried out using a Tecmag Redstone NMR spectrometer, (Houston, TX) connected to a 0.09 T SMIS electromagnet with a home-built NMR probe equipped with an rf coil tuned and matched to the $\omega_o/2\pi = 4$ MHz ^{1}H Larmor frequency. This magnet will be referred to as the 4 MHz electromagnet in subsequent sections. Values for T_1 were determined using a 21-step inversion recovery experiment with recovery times ranging nonlinearly between 0 and 300 ms, while T_2 values were measured using a Carr–Purcell–Meiboom–Gill (CPMG) pulse sequence (Carr & Purcell, 1954; Hoult & Richards, 2011; Meiboom & Gill, 1958).

In order to make the method factory deployable, three portable, low-resolution, single-sided instruments were compared. The first sensor, which will be referred to as the 5.25 MHz magnet, is a 45 × 45 × 16 cm, 0.12 T barrel permanent magnet with a surface coil tuned to $\omega_o/2\pi = 5.25$ MHz (McDowell & Fukushima, 2008; Utsuzawa & Fukushima, 2017). For this magnet, the volume of maximum static magnetic field homogeneity or "sweet spot" standoff is 0.5 cm above the magnet surface. The second sensor,

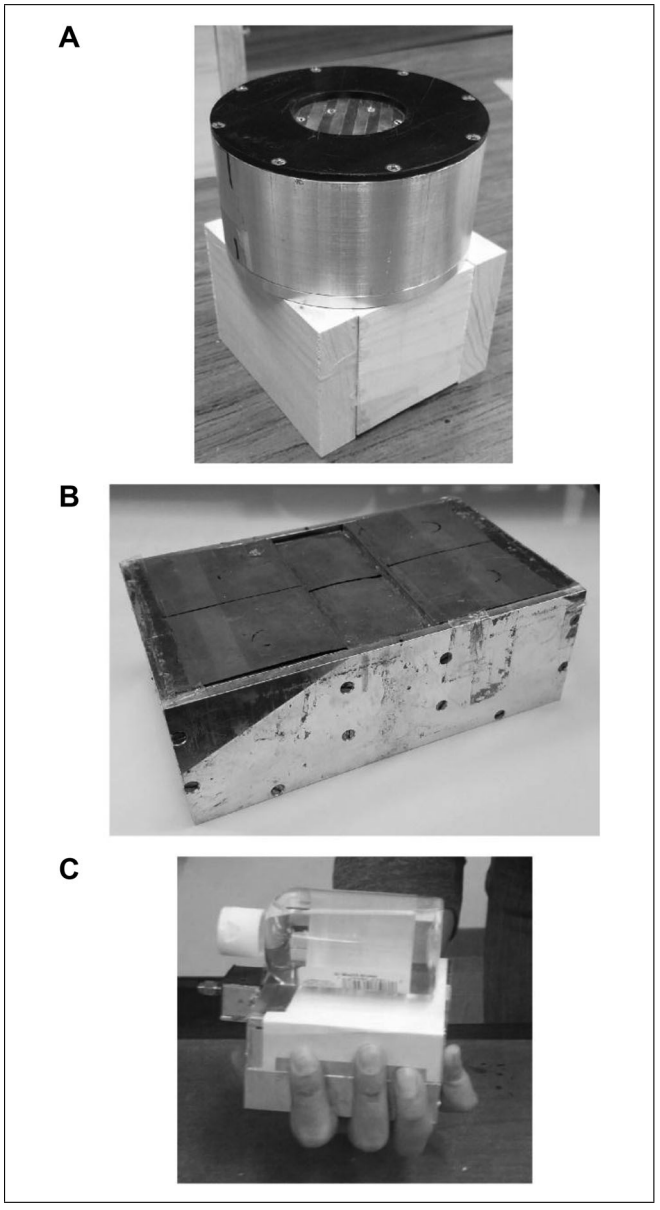

Figure 1–Photographs of the 5.25 MHz barrel permanent magnet with a penetration depth of 0.5 cm (A), the 2.28 MHz unilateral permanent magnet with a penetration depth of 2.5 cm (B), and the 19.5 MHz unilateral permanent magnet with a penetration depth of 4 mm (C).

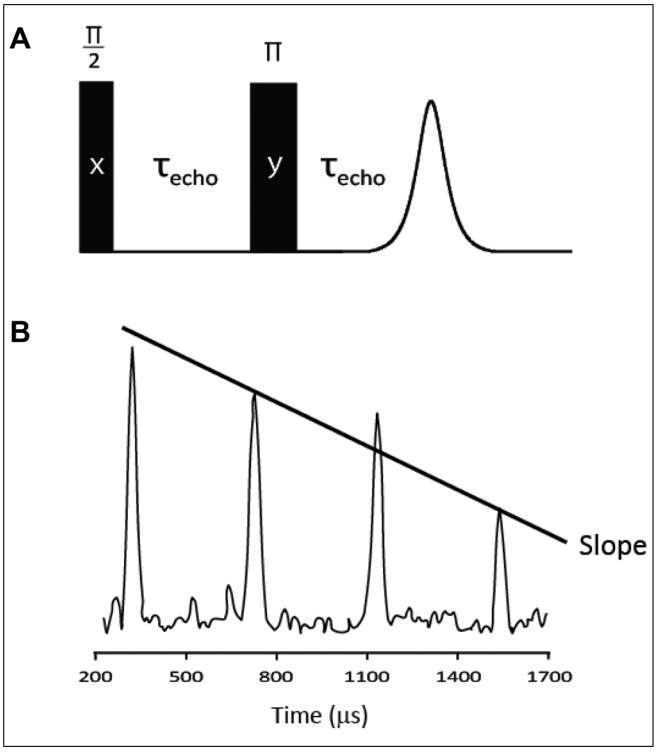

Figure 2–(A) Spin echo pulse sequence used for the echo slope measurement where four values of τ_{echo} are used to obtain a slope estimate; (B) an example of the four echoes obtained using the 19.5 MHz magnet for four choices of τ_{echo}; the straight solid line shows the fit of each spin echo maximum value to a straight line.

Table 2–Percentage of glycerin and viscosity of glycerin/water samples reproduced from Sheely (1932).

%Glycerin	Viscosity (cP)
100	945
96	435
90	164
85	82
78	38
72	21
62	10
45	4
30	2
10	1
0	0

referred to as the 2.28 MHz magnet hereafter, is a 18 × 11 × 7 cm, 0.05 T unilateral permanent magnet with a homogeneous sweet spot 2.5 cm off the magnet surface (Garcia-Naranjo, Guo, Marica, Liao, & Balcom, 2014; Marble, Mastikhin, Colpitts, & Balcom, 2007). A $\omega_o/2\pi$ = 2.28 MHz homebuilt surface coil designed for the 0.05 T magnet allows the sweet spots of the rf and static magnetic fields to coincide 2.5 cm above the magnet surface (Casanova, Perlo, & Blumich, 2011). The final sensor, which will be referred to as the 19.5 MHz magnet hereafter, is a 10 × 11 × 5 cm, 0.46 T permanent magnet equipped with a flat rf surface coil that is tuned and matched to $\omega_o/2\pi$ = 19.5 MHz and a sweet spot standoff of 4 mm. A photograph of each of the magnets is provided in Figure 1. All of the magnets were controlled in the factory with a portable, COSA Xentaur, (Houston, TX) SpinPulse Model CX-20 spectrometer.

Observed transverse magnetization decay rate values $1/T_2^{obs}$ were measured on all three magnets using the CPMG pulse sequence. In some cases, faster spoilage detection was achieved by the acquisition of four spin echoes with the delay times between the $\pi/2$ and π pulses being τ_{echo} = 300, 700, 1,100 and 1,500 μs. The amplitude of these echoes as a function of τ_{echo} was fit to a line and the slope was used to characterize spoilage. This approach, referred to as the echo slope measurement, as shown in Figure 2, is more sensitive to subtle changes in viscosity or diffusion than the CPMG pulse sequence as the unequal pulse delay times for the individually measured spin echoes do nothing to attenuate the effects of diffusion. The equal pulse delay times in the CPMG sequence attenuate the effects of viscosity on the measured signals. CPMG and echo slope measurements were obtained for the glycerin/water samples in Table 2 using all three single-sided instruments. Viscosities for glycerin/water test

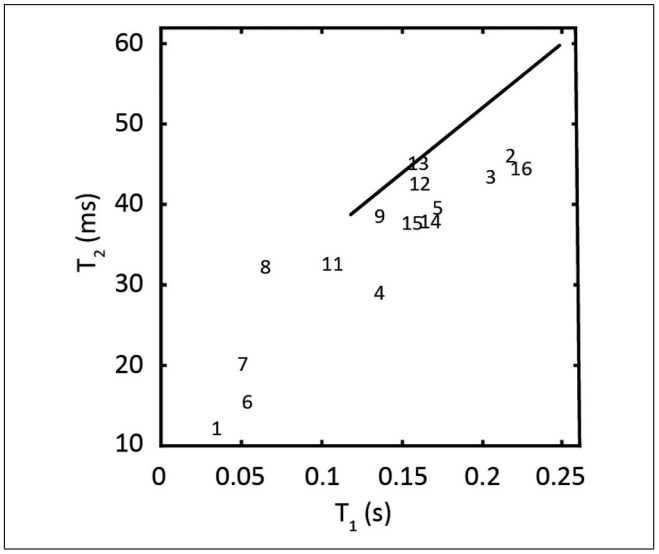

Figure 3–Measured T_1 values plotted against measured T_2 values for wild-type tomato concentrate samples; the numbers correspond to the sample codes listed in Table 1, and the center of the number in the plot communicates the measured T_1 and T_2 values. The solid line indicates the values determined for pristine tomato concentrate samples. It should be noted that sample 10 is not shown because the 0.5 s T_1 value is off the plot scale.

samples made according to Sheely (1932) are shown in Table 2. All the reported averages and standard deviations correspond to triplicate measurements unless otherwise stated.

Results and Discussion

The high-resolution 4 MHz electromagnet was used to study the effects of different spoilage mechanisms on NMR relaxation times. Contrary to the expectation based on previous studies, the T_1 and T_2 values measured for the wild-type samples did not change over the 40 days of measurement (Pinter et al., 2014). However, the measured T_1 and T_2 values of the wild-type samples differed from the T_1 and T_2 values measured for the pristine samples having the same %NTSS. The measured T_1 and T_2 values of the pristine samples were linearly related to the %NTSS, as shown by the line in Figure 3. The pristine samples with larger %NTSS values had smaller T_1 and T_2 values. The results suggest that all wild-type samples, except for sample 13, were spoiled upon delivery. The presence of mold growth on the samples reinforced the conclusion that all samples were spoiled. As mentioned above, previous work showed that T_1 values increase for 5 days after inoculation with microorganisms, after which the T_1 values remain relatively constant (Pinter et al., 2014). If the wild-type samples were initially exposed to a contaminant more than 5 days before arrival, no drastic increase in the T_1 or T_2 values would have been expected over the course of the study. During the process of spoilage, the viscosity of tomato concentrate can change as it is broken down by fermentation caused by lactic acid bacteria (Arkoun, Abbas, & T. K., 2015; Juven & Weisslowicz, 1981; Mallidis & Samaras, 1987; Schaffner & Beuchat, 1986). Other spoilage detection methods involve measuring the viscosity of the sample; however, these methods require that the container be opened for analysis. It is well known that T_1 and T_2 values are inversely related to the viscosity of the sample, so that a change in viscosity upon spoilage results in change in the measured T_1 and T_2 values. As mentioned above, the %NTSS, or the concentration of solid tomato product in the liquid serum, is directly related to the viscosity of the tomato concentrate (Hayes, Smith, & Morris, 1998; McCarthy et al., 2008); thus, a sample with a higher %NTSS is expected to have T_1 and T_2 values that are smaller than those of a sample having lower %NTSS, consistent with the solid line in Figure 3. Wild-type samples with the same labeled %NTSS values did not provide the same T_1 and T_2 values. It should be noted that the stored %NTSS measured before the delivery of the samples and shown in Table 1 is different from the prepared, expected %NTSS for most samples. Again, this suggests that the samples displayed a change in viscosity upon spoilage and may have been spoiled upon arrival.

In addition to the dependence of the inherent T_2 value on the viscosity of the sample, the observed relaxation time value also depends on the strength of the magnetic field gradient produced by the NMR magnet. For the CPMG pulse sequence, the observed relaxation rate $1/T_2^{obs}$ can be separated into the inherent spin–spin relaxation rate $1/T_2$ and the inhomogeneous field, diffusion-dependent rate $1/T_2^{D}$ as

$$\frac{1}{T_2^{obs}} = \frac{1}{T_2} + \frac{1}{T_2^{D}} \quad (2)$$

The diffusion dependent rate reduces to $1/T_2^{D} = (\gamma G \tau_{echo})^{2} D/3$, where γ is the gyromagnetic ratio, D is the diffusion coefficient, and G is the strength of an applied linear, single-axis magnetic field gradient G. In low resolution, single-sided NMR instruments G can be large enough so that $1/T_2^{D}$ dominates $1/T_2$ in Eq. (2), and the overall measured $1/T_2^{obs}$ will reflect diffusion and macroscopic transport, not spin–spin relaxation. In high-resolution instruments, such as the 4 MHz electromagnet described above, the magnetic field is very homogeneous. As a result, $1/T_2^{D}$ is small and $1/T_2^{obs}$ reflects spin–spin relaxation, not macroscopic transport.

In order to gauge the magnetic field inhomogeneity contributions to $1/T_2^{obs}$ in real experiments on the three portable magnets, CPMG measurements were obtained for the 11 glycerin/water samples described in Table 2. Measurements of $1/T_2$ were first collected with the high-resolution 4 MHz electromagnet using short τ_{echo} values in the CPMG pulse sequence. The solid line in Figure 4 captures the average measured $1/T_2^{obs}$ values for the sample set in Table 2 while the shaded region reports on the standard deviation in each average value. Since the 4 MHz electromagnet has a homogenous field, as evidenced by the 20 Hz linewidth displayed upon Fourier transformation of the free induction signal following a single rf pulse, the $1/T_2^{obs}$ values shown in Figure 4 are the inherent spin–spin relaxation rate values $1/T_2$. The relaxation rate trend shown in Figure 4 is exactly what one expects for glycerin/water mixtures. The large relaxation rate at large viscosity >100 cP or small D value corresponds to solutions composed mostly of glycerin, with a small amount of water. It is the short T_2 = 10 ms value for pure glycerin that makes this rate large. The small relaxation rate at low viscosity or large D value corresponds to solutions composed mostly of water, with a small amount of glycerin. It is the long T_2 = 2.4 s value for pure water that makes this rate small. Similar CPMG estimates of $1/T_2^{obs}$ were obtained for the sample set in Table 2 using the three single-sided magnets. The solid line and shaded region bracketing that line in Figure 5 again communicate the average and standard deviation of the $1/T_2^{obs}$ value for a given sample viscosity. The dashed line shown in the plots in Figure 5 is $1/T_2^{D} = 1/T_2^{obs} - 1/T_2$, where the $1/T_2$ value for each sample viscosity is obtained from Figure 4. The shaded regions surrounding the dashed line again represent the standard

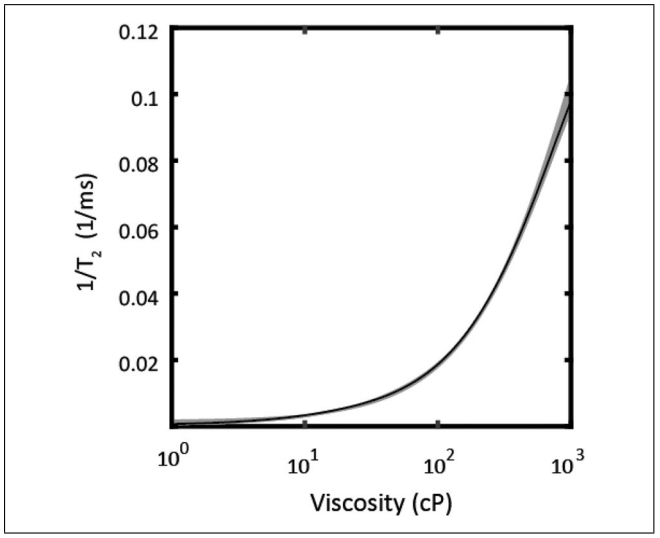

Figure 4–CPMG decay rates for the glycerin/water samples shown in Table 2 obtained from the high-resolution 4 MHz electromagnet; the average rate is communicated by the solid line while the shaded region captures the standard deviation of the average measured values.

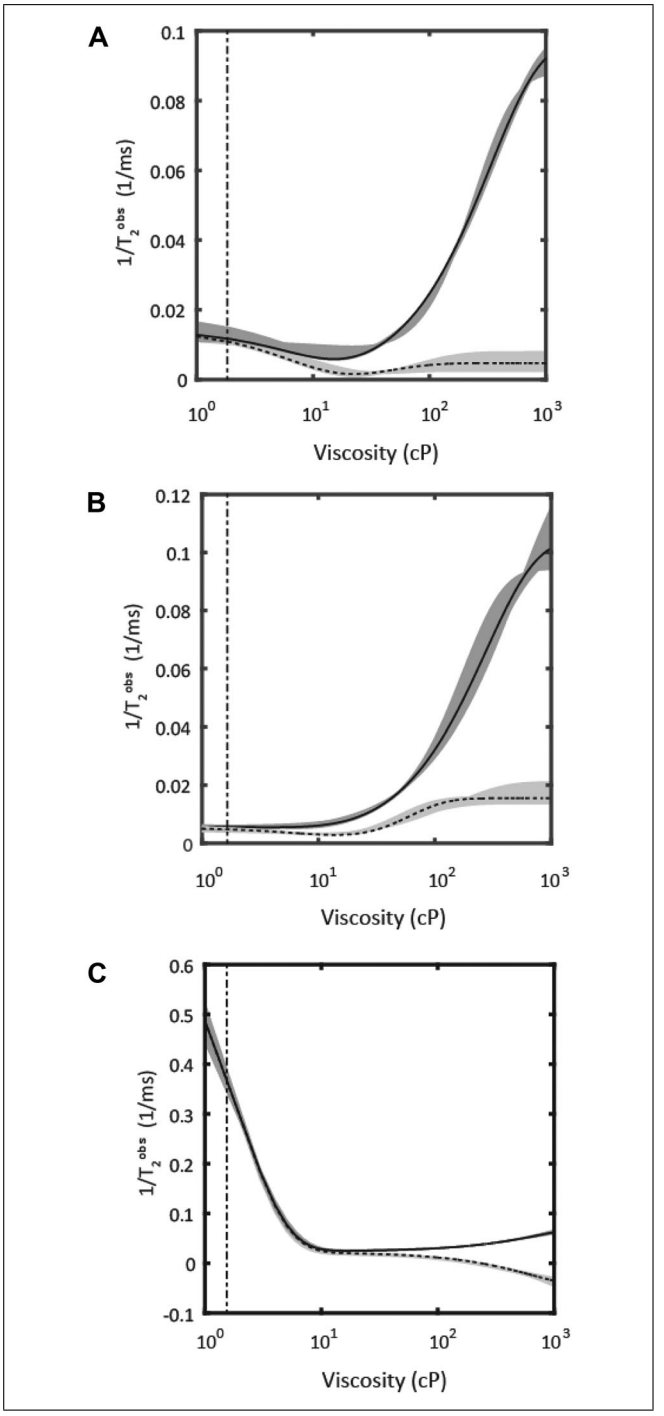

Figure 5–CPMG decay rates for the glycerin/water solutions obtained from the 5.25 MHz magnet (A), the 2.28 MHz magnet (B), and the 19.5 MHz magnet (C); the solid line communicates the average measured value, while the shaded regions show the standard deviations in the measurements. The dashed line communicates the diffusion dependent rate term $1/T_2^D$. The dot, dashed vertical lines indicate the average tomato concentrate viscosity.

deviation in the calculated $1/T_2^D$ values. Consider first the similarities between the results shown for the three separate magnets in Figure 5. At very high viscosity, that is, >100 cP in Figure 5, $1/T_2^{obs}$ is dominated by inherent T_2 relaxation as $1/T_2^{obs} \gg 1/T_2^D$ in this limit. Since $1/T_2^D \propto D$, the diffusion contributions to $1/T_2^{obs}$ become smaller with increasing viscosity because the D value decreases. The opposite trend appears at low viscosity <10 cP in Figure 5. Here, $1/T_2^{obs}$ is dominated by diffusion as $1/T_2^{obs} \approx 1/T_2^D \gg T_2$ in this limit and the solid and dashed lines in Figure 5 overlap. Now consider the differences between the results shown for the three separate magnets in Figure 5. The behavior of the 5.25 MHz and 2.28 MHz magnets in Figure 5(A) and 5(B) is similar, as expected based on the construction of the magnets (Garcia-Naranjo et al., 2014; Marble et al., 2007; McDowell & Fukushima, 2008; Utsuzawa & Fukushima, 2017). These two magnets were designed to provide a large homogenous magnetic field volume displaced at a fixed distance from the magnet surface. Although still inhomogeneous by high-resolution NMR standards, the magnetic field homogeneity in these surface displaced volumes is high enough to attenuate the effects of $1/T_2^D$ by keeping the magnetic field gradients G small. A similar argument cannot be applied to the 19.5 MHz magnet, where similar design efforts were not made. Here, the magnetic field is grossly inhomogeneous, the G value in the sensitive volume is large, and diffusion completely dominates the measured response. This effect is illustrated at low viscosity <10 cP, and thus high D value when comparing Figure 5(C) to Figure 5(A) and 5(B).

An effective tomato concentrate spoilage detector must be able to discriminate between samples with slightly different viscosity or D values. The slope of the $1/T_2^{obs}$ curves in Figure 5 can be used to decide which magnet provides the best viscosity discrimination. The dot, dashed vertical lines in each of the plots in Figure 5 label the viscosity for typical pristine tomato concentrate. Since tomato concentrate spoilage detection relies on monitoring of T_2 values, the results shown in Figure 5 suggest that a measurement of T_2^{obs} will provide a way to accomplish this goal as it is the small changes to the tomato concentrate viscosity due to spoilage that are observed. Since actual tomato concentrate measurements will be restricted to a small range of viscosities around the dot, dashed vertical lines in the plots in Figure 5, it appears that the 19.5 MHz magnet will be the most sensitive tomato concentrate spoilage detector as it displays the largest slope. The negatively sloped straight $1/T_2^{obs}$ line and the similarity between $1/T_2^{obs}$ and $1/T_2^D$ in Figure 5(C) at low viscosity suggest that diffusion

dominates CPMG relaxation rate measurements obtained with the 19.5 MHz magnet. The negative slope is consistent with diffusion-dominated relaxation as $1/T_2^D$ linearly depends on D. As viscosity decreases, the D value increases and $1/T_2^D$ becomes larger. The dramatic low viscosity difference between the $1/T_2^{obs}$ behavior in Figure 5(C) and Figure 5(A) and 5(B) due to the large field gradient inherent to the 19.5 MHz magnet is what suggests the spin echo slope measurement shown in Figure 2. The echo slope approach shown in Figure 2 measures four spin echoes with four different τ_{echo} choices. In the case of low and moderate magnetic field inhomogeneity, the argument of the exponential damping function describing each spin echo is $2\gamma^2G^2D\tau_{echo}^3/3$ in the special case where a single linear gradient is applied. The situation is different in very broad line situations where large field gradients or fast motion is present. Here, the argument of the exponential function changes to $(2\gamma^2G^2L^4/D)\tau_{echo}$ (Herzog & Hahn, 1956; Riley, Vyas, & Augustine, 2001), where L is the sample length. In the limit that τ_{echo} is small and D is large, the spin echo damping function can be linearized to $1 - (2\gamma^2G^2L^4/D)\tau_{echo}$ and the slope $2\gamma^2G^2L^4/D$ can be used to discriminate between samples of different mobility, viscosity, or, in this case, spoilage amount via the slope dependence on D value.

The plots in Figure 6 show how the spin echo slope changes for the different viscosity samples in Table 2 using the same three single-sided magnets. The solid line again communicates the average slope at each viscosity while the shaded region indicates the standard deviation in the average slope. The results in Figure 6(A) and 6(B) for the carefully designed 5.25 MHz and 2.28 MHz magnets are again different from those for the large gradient 19.5 MHz magnet. The larger standard deviation in Figure 6(A) and 6(B) at all viscosities in comparison to Figure 6(C) is expected as the higher magnetic field presented by the 19.5 MHz magnet provides a greater signal-to-noise ratio for the same amount of signal averaging. The difference in the functional forms of the responses between Figure 6(A) and 6(B) and the large gradient magnet response in Figure 6(C) is also expected. The results for the 19.5 MHz magnet at low viscosity in Figure 6(C) are better described by a spin echo damping function dependent on τ_{echo} where response linearization is sensible. On the other hand, the results for the 5.25 MHz and 2.28 MHz magnets at all viscosities are best described by a damping function dependent on τ_{echo}^3 where response linearization with respect to τ_{echo} is not as sensible and leads to the complicated functional dependence shown in Figure 6(A) and 6(B). In spite of the differences between the three magnet responses shown in Figure 6 across the entire viscosity range, the response of each magnet near the average viscosity for tomato concentrate, indicated by the dot, dashed vertical lines in the plots in Figure 6, is similar. Moreover, the value and slope of the echo slope response at the viscosity appropriate for tomato concentrate in Figure 6 are larger than the corresponding values obtained with the CPMG approach in Figure 5. This strongly suggests that the instrumentally less demanding and time-efficient echo slope approach is more sensitive to small motional changes and thus tomato concentrate spoilage than the standard CPMG method when using single-sided magnets. Indeed, a comparison of the slopes at the average tomato concentrate viscosity, shown by the dot, dashed vertical lines in Figure 6, for each magnet reveals that the 19.5 MHz magnet provides the best sensor for discriminating between pristine and spoiled tomato concentrate.

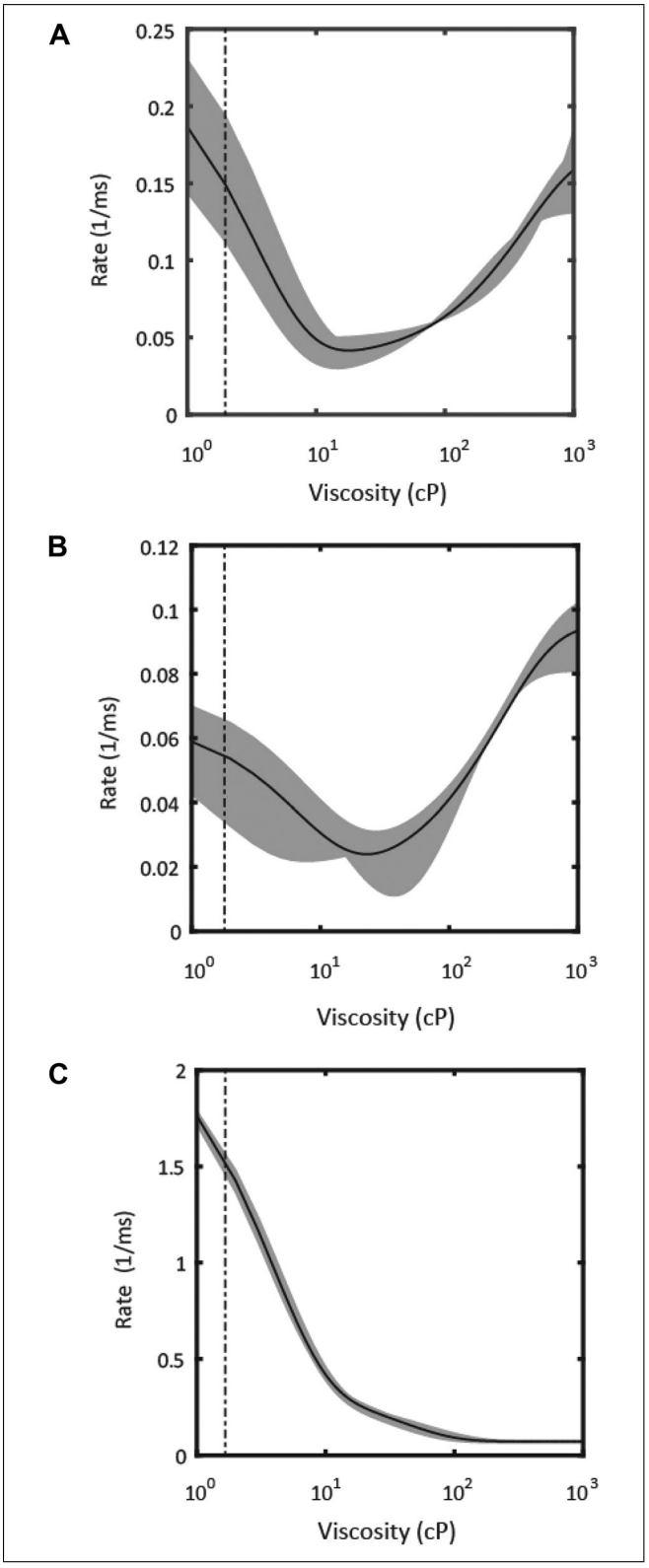

Figure 6–Echo slope measurements for the glycerin/water solutions obtained from the 5.25 MHz magnet (A), the 2.28 MHz magnet (B), and the 19.5 MHz magnet (C); the average echo slope value is communicated by the solid line, while the shaded region captures the standard deviation of these average measured values. The dot, dashed vertical lines indicate the average tomato concentrate viscosity.

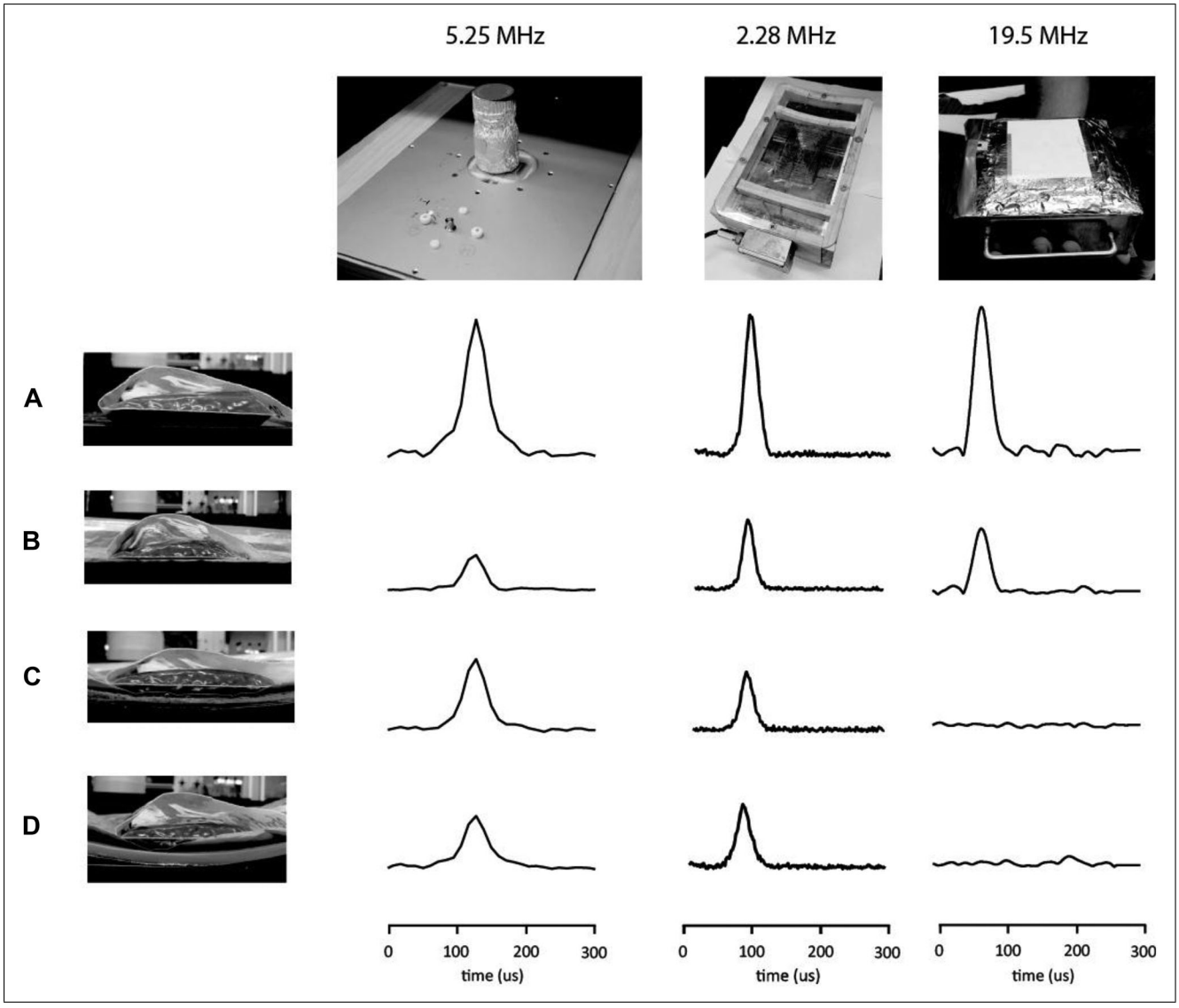

Figure 7–Spin echo signals from each of the three magnets as a function of the material placed between the magnet and the tomato concentrate sample; there is no material (A), an aseptic metal bag layer (B), a 0.5-cm thick cardboard bin section and aseptic packaging layer (C), and a 0.5-cm thick plastic bin section and aseptic package (D).

Although it appears that the 19.5 MHz magnet provides the best discrimination between samples of different viscosity, it is important to remember that an effective tomato concentrate spoilage sensor must also be able to detect spoilage through the 0.5 to 4 cm thick plastic, cardboard, or wooden bins that house the tomato concentrate during storage. Figure 7 compares the spin echo signals obtained from the three magnets considered here as a function of material placed between the sample and the magnet. The rows from top to bottom in Figure 7 correspond to no material, aseptic package material, cardboard bin and aseptic material, and plastic bin and aseptic material between the sample and the magnet. While the 19.5 MHz single-sided magnet, with a standoff of only 4 mm, does not allow for signal acquisition through the bins with >0.5 cm wall thickness, the 5.25 MHz barrel magnet and the 2.28 MHz unilateral magnet allow for signal acquisition through the factory-relevant containers. The 2.28 MHz unilateral magnet has a sweet spot standoff 2.5 cm off the surface of the magnet, allowing for the greatest penetration depth of the magnetic field in the sample.

The temperature stability of the magnet is also important when developing an effective sensor. The tomato concentrate is stored outside year round; therefore, the temperature of the sensor varies based on the weather. With drastic temperature changes, there was a loss of signal from the 5.25 MHz magnet unless the Larmor frequency was manually changed. Specifically, after leaving the instrument outside overnight in the middle of Northern Californian winter, where a modest temperature of 10 °C is common, NMR signals could not be observed. In this case, the rf frequency had to be increased by 20 kHz in order to regain signal. It is not practical to determine the correct frequency on a bin-to-bin and/or day-to-day basis in a factory environment. By comparison, the performance of the 2.28 MHz magnet was stable in the 10 to 30 °C temperature range.

The ideal instrument for a tomato concentrate spoilage sensor that produces the largest measurable difference in tomato concentrate viscosity has a sweet spot standoff of >0.5 cm similar to the 2.28 MHz and 5.25 MHz magnets, is temperature stable similar to the 2.28 MHz magnet, and has a large rf and dc gradient

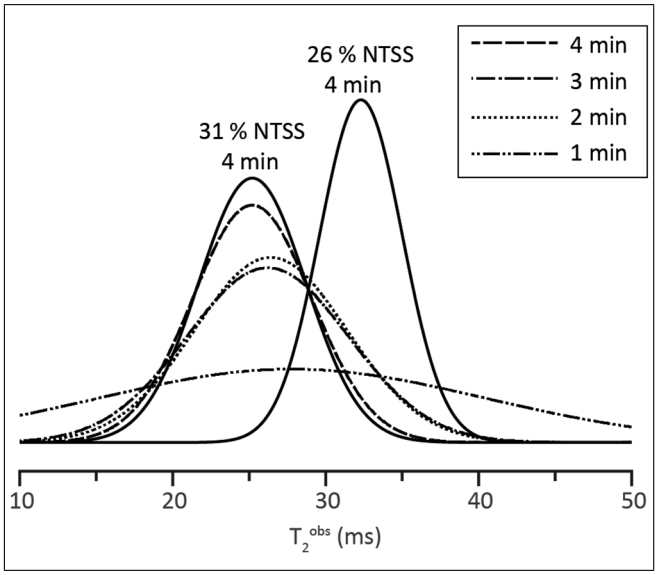

Figure 8–Summary of experimental results used to optimize tomato concentrate spoilage detection in real factory located bins with the 2.28 MHz unilateral magnet; the solid black lines capture the T_2^{obs} values for pristine 31 %NTSS and 26 %NTSS samples when 200 averages that take 4 min of signal averaging are used. The peak maxima correspond to the average measured T_2^{obs} value while the peak width communicates the standard deviation in the average T_2^{obs} value. Experience and Figure 4 dictate that the ability to distinguish between these two %NTSS samples is critical for tomato concentrate spoilage detection. The other peaks for the 31 %NTSS sample for 1, 2, 3, and 4 min of signal averaging suggest that just 2 min of signal averaging is all that is required to detect spoiled tomato concentrate.

similar to the 19.5 MHz magnet. Although the 2.28 MHz unilateral magnet does not provide the greatest tomato concentrate spoilage discrimination, it is remarkably temperature stable and has adequate stand-off for factory studies. Consequently, the 2.28 MHz unilateral magnet was modified and used to study tomato concentrate bins at the factory over a 1-year period. During this time, the sheer number of bins studied required that an optimum throughput rate be identified to maximize spoilage screening efficiency. NMR signal averaging is by far the most time-consuming aspect of the spoilage detection process. Echo train signals resulting from 1-min long (50 scans) CPMG experiments were summed to simulate experiments of 1, 2, 3, and 4 min. Comparison of the average decay time constant values and their standard deviations over 100 repeat experiments can be used to construct a Gaussian peak that labels the average T_2^{obs} value by position and the standard deviation of these values by width, as shown in Figure 8. As expected, more signal averages reduce noise and increase confidence in the T_2^{obs} value manifest as a narrowing of the Gaussian peak and an increase in resolution of the tomato concentrate spoilage detection. The results in Figure 8 suggest that 2-min long experiments (100 scans) give reproducible CPMG decay rates and allow for the shortest spoilage detection measurements. A broader range of decay rates were measured for shorter experiments due to the presence of more noise in the data and similar results were obtained for the spin echo slope approach.

Conclusion

A viscosity-dependent NMR parameter that takes advantage of the inhomogeneity inherent to single-sided NMR sensors has been shown to successfully determine tomato concentrate spoilage in a factory-relevant environment. The most effective tomato concentrate spoilage detector has rf and static magnetic field gradients that are large enough so that the echo slope method presented here discriminates between small changes in tomato concentrate viscosity. The instrument must be temperature stable and have a large enough standoff to detect spoilage through the aseptic bags and large-volume factory containers. For these reasons, a 2.28 MHz unilateral magnet is currently being used at a tomato concentrate packaging facility to screen tomato concentrate bins. Future work will include the development and configuration of multiple robust sensors that will allow for the simultaneous screening of multiple bins in a factory environment. This approach and sensor is not limited to tomato products and can be used to study anything in a sealed metallic or nonmetallic container. The advantages of this sensor are the low cost, portability, and the range of aseptic container sizes and geometries that can easily be tested for spoilage.

Acknowledgments

The authors gratefully acknowledge the support for this work provided by the California League of Food Processors. A rich collaboration with Cosa Xentaur and valuable conversations with Paul Giammatteo and Eichi Fukushima are also gratefully acknowledged.

Author Contributions

M. N. Martin customized all of the NMR equipment for factory deployment, performed all of the experiments, analyzed all of the data, and helped with manuscript preparation. B. J. Balcom designed and provided the 2.28 MHz unilateral magnet and helped draft the manuscript. M. J. McCarthy helped design the instrument for factory deployment and participated in manuscript preparation. M. P. Augustine is the PI and corresponding author, and had a role in each and every aspect of the work.

References

Adilettaa, G., Russob, P., Proiettic, N., Capitanic, D., Manninad, L., Crescitellie, A., & Di Matteoa, M. (2015). Characterization of pears during drying by conventional technique and portable non invasive NMR. *Chemical Engineering Transactions*, *44*, 151–156. https://doi.org/10.3303/CET1544026

Arkoun, F. C., Abbas, D. K., & T. K, Z. (2015). Evaluation of lactic acid bacteria isolated from fermented tomatoes to produce antimicrobial activities against several bacteria and fungi. *Advances in Food Science and Technology*, *3*(8), 332–338.

Augustine, M. P., Lim, V., & Broz, J. S. (2016). Methods and apparatus for analysis of sealed containers. U.S. Patent No. US2016/0003753 A1.

Carr, H. Y., & Purcell, E. M. (1954). Effects of diffusion on free precession in nuclear magnetic resonance experiments. *Physical Review*, *94*(3), 630–638. https://doi.org/10.1103/PhysRev.94.630

Casanova, F., Perlo, J., & Blumich, B. (2011). *Single-sided NMR*. New York: Springer. DOI: 10.1007/978-3-642-16307-4

Celozzi, S., Rodolfo, A., & Lovat, G. (2008). *Electromagnetic shielding*. Hoboken, NJ: John Wiley & Sons Inc. https://doi.org/10.1002/9780470268483

Concina, I., Falasconi, M., Gobbi, E., Bianchi, F., Musci, M., Mattarozzi, M., . . . Sberveglieri, G. (2009). Early detection of microbial contamination in processed tomatoes by electronic nose. *Food Control*, *20*(10), 873–880. https://doi.org/10.1016/j.foodcont.2008.11.006

Garcia-Naranjo, J. C., Guo, P., Marica, F., Liao, G., & Balcom, B. J. (2014). Magnetic resonance core-plug analysis with the three-magnet array unilateral magnet. *Petrophysics*, *55*(3), 229–239.

Gould, W. A. (2013). *Tomato production, processing and technology*. Amsterdam: Elsevier.

Guthausen, A., Guthausen, G., Kamlowski, A., Todt, H., Burk, W., & Schmalbein, D. (2004). Measurement of fat content of food with single-sided NMR. *Journal of the American Oil Chemists' Society*, *81*(8), 727–731. https://doi.org/10.1007/s11746-004-0969-5

Hayes, W. A., Smith, P. G., & Morris, A. E. J. (1998). The production and quality of tomato concentrates. *Critical Reviews in Food Science and Nutrition*, *38*(7), 537–564. https://doi.org/10.1080/10408699891274309

Herzog, B., & Hahn, E. L. (1956). Transient nuclear induction and double nuclear resonance in solids. *Physical Review*, *103*(1). 148–166. https://doi.org/10.1103/PhysRev.103.148

Hoult, D. I., & Richards, R. (2011). The signal-to-noise ratio of the nuclear magnetic resonance experiment. *Journal of Magnetic Resonance*, *213*(2), 329–343. https://doi.org/10.1016/j.jmr.2011.09.018

Juven, B. J., & Weisslowicz, H. (1981). Chemical changes in tomato juices caused by lactic acid bacteria. *Journal of Food Science*, *46*, 1543–1545. https://doi.org/10.1111/j.1365-2621.1981.tb04216.x

Luster, C. (1978). A rapid and sensitive sterility monitoring technique for aseptically processed bulk tomato paste. *Journal of Food Science*, *43*, 1046–1048. https://doi.org/10.1111/j.1365-2621.1978.tb15228.x

Mallidis, C. G., & Samaras, F. (1987). A simple, rapid and sensitive method for monitoring contamination of aseptically processed tomato paste. *International Journal of Food Science and Technology*, *22*, 59–66. https://doi.org/10.1111/j.1365-2621.1987.tb00456.x

Marble, A. E., Mastikhin, I. V., Colpitts, B. G., & Balcom, B. J. (2007). A compact permanent magnet array with a remote homogeneous field. *Journal of Magnetic Resonance*, *186*, 100–104. https://doi.org/10.1016/j.jmr.2007.01.020

McCarthy, K. L., Sacher, R. F., & Garvey, T. C. (2008). Relationship between rheological behavior and Bostwick measurement during manufacture of ketchup. *Journal Texture Studies*, *39*(5), 480–495. https://doi.org/10.1111/j.1745-4603.2008.00155.x

McDowell, A., & Fukushima, E. (2008). Ultracompact NMR: 1 H spectroscopy in a sub-kilogram magnet. *Applied Magnetic Resonance*, *35*(1), 185–195. https://doi.org/10.1007/s00723-008-0151-3

Meiboom, S., & Gill, D. (1958). Modified spin-echo method for measuring nuclear relaxation times. *Review of Scientific Instruments*, *29*(8), 688–691. https://doi.org/10.1063/1.1716296

Petrov, O. V., Hay, J., Mastikhin, I. V., & Balcom, B. J. (2008). Fat and moisture content determination with unilateral NMR. *Food Research International*, *41*(7), 758–764. https://doi.org/10.1016/j.foodres.2008.05.010

Pinter, M. D., Harter, T., McCarthy, M. J., & Augustine, M. P. (2014). Towards using NMR to screen for spoiled tomatoes stored in 1,000 L, aseptically sealed, metal-lines totes. *Sensors*, *14*, 4167–4176. https://doi.org/10.3390/s140304167

Riley, S. A., Vyas, S., & Augustine, M. P. (2001). Motional smearing of electrically recovered couplings measured from multipulse transients. *Concepts in Magnetic Resonance*, *13*(3), 171–189. https://doi.org/10.1002/cmr.1007

Schaffner, D. W., & Beuchat, L. R. (1986). Fermentation of aqueous plant seed extracts by lactic acid bacteria. *Applied and Environmental Microbiology*, *51*(5), 1072–1076.

Schenz, T. W., Courtney, K. L., Israel, B. R., & Reaves, L. A. (1993). Non-destructive detection of spoilage using nuclear magnetic resonance spectroscopy. U.S. Patent No. 5, 270, 650.

Sheely, M. L. (1932). Glycerol viscosity tables. *Industrial and Engineering Chemistry*, *24*, 1060–1064. 10.1021/ie50273a022

Utsuzawa, S., & Fukushima, E. (2017). Unilateral NMR with a barrel magnet. *Journal of Magnetic Resonance*, *282*, 104–113. https://doi.org/10.1016/j.jmr.2017.07.006

Veliyulin, E., Mastikhin, I. V., Marble, A. E., & Balcom, B. J. (2008). Rapid determination of the fat content in packaged dairy products by unilateral NMR. *Journal of the Science of Food and Agriculture*, *88*(14), 2563–2567. https://doi.org/doi.org/10.1002/jsfa.3391

Veliyulin, E., van der Zwaag, C., Burk, W., & Erikson, U. (2005). In vivo determination of fat content in Atlantic salmon (Salmo salar) with a mobile NMR spectrometer. *Journal of the Science of Food and Agriculture*, *85*(8), 1299–1304. https://doi.org/doi.org/10.1002/jsfa.2117

Xu, Z., Morris, R. H., Bencsik, M., & Newton, M. I. (2014). Detection of virgin olive oil adulteration using low field unilateral NMR. *Sensors*, *14*(2), 2028–2035. https://doi.org/10.3390/s140202028